P6.10

TURBULENCE OBSERVATIONS AT THE EDGE OF A CLIFF

Otávio C. Acevedo[1], Osvaldo L. L. Moraes, Rodrigo da Silva
Universidade Federal de Santa Maria, Santa Maria, RS, Brazil

1. INTRODUCTION

a

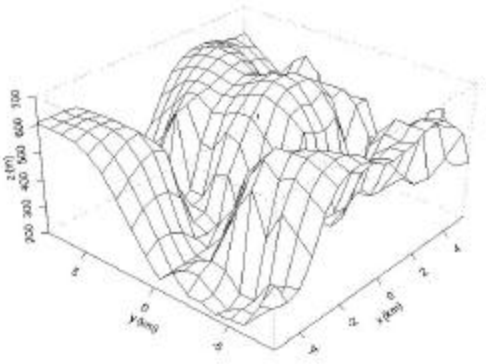

b

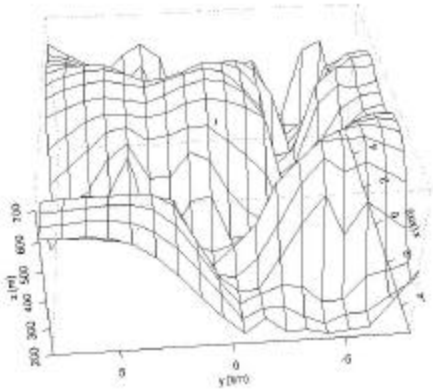

Figure 1. Two different views of the local topography, North-south direction corresponds to “y” axis. The tower is shown (to scale) as a small black segment in the middle of each panel.

Only in recent years attention has been devoted to the structure of atmospheric turbulence over very complex terrain. Rotach et. al. (2000) describe an extensive field program, the MAP Riviera project, in which turbulence was measured both at the bottom and at the slopes of an alpine valley. The vast majority of observational campaigns in the boundary layer were conducted in flat, horizontally-homogeneous terrains (e.g., Kansas project; Haugen et. al., 1971). The interpretation of flux observations over homogeneous surfaces is simpler, as in this case there is no need of the identification of the flux footprint, i.e., that portion of the surface contributing to the quantities measured by the tower.

In the present study, we describe flux observations taken at the edge of a sharp cliff (figure 1), at the bottom of which a river (Rio das Antas) runs. The steep slope starts only a few meters from the tower, at its west side. Another sharp cliff exists at 1 km, south of the tower, as is apparent in figure 1b. The analysis of the observations has to consider not only the spatial heterogeneity, but also the extreme topography, which affects the turbulent field and energy partition at the site. We show mean fields and surface fluxes measured at the tower. The analysis is mainly focused on the average daily evolution of these quantities over clear days (10 cases).

2. THE REGION AND OBSERVATIONS

An intensive observational campaign was conducted at Nova Roma do Sul (29°01´22´´S, 51°26´38´´W), located in the mountainous area of southern Brazil (Serra Geral, figure 2) from 5 November 2001 to 15 December 2001. The effort aims toward understanding the physical microclimatology of the region, which will be partially flooded in the upcoming years due to the construction of three dams. In the future, the measurements presented here will feed mesoscale circulation models that will simulate the climatic impact of the flooding.

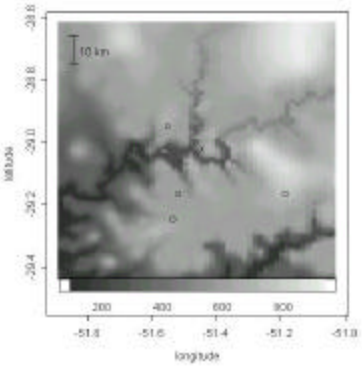

Figure 2. Topography of the region, given by gray scale at the bottom. The site is indicated by an “x”. Circles show the position of nearby towns.

[1] Corresponding author address Otávio C. Acevedo, Universidade Federal de Santa Maria, Departamento de Física/ CCNE, Santa Maria, RS, Brazil, 97105-900
email: otavioa@yahoo.com

The measurements were taken at a 15-m high micrometeorological tower, containing three levels (3.7, 5.8 and 8.9 m) of mean winds, temperature and humidity. Turbulence was measured at 14 m by a 3D sonic anenometer and a krypton hygrometer. Net radiation, incident short wave radiation, soil heat flux and three levels of soil temperatures were also measured.

3. RESULTS

3.1. *Mean winds*

The local circulations at the site are totally controlled by the topography. Classical mountain-valley circulations are observed (figure 3). Upslope winds exist from 1100 LST to 1800 LST, and the mean streamline reaches a maximum angle of 18.5° with the horizontal, at 1500 LST (figure 4). Nocturnal, downslope winds are much weaker than the daytime ones, with the largest wind magnitudes being observed near sunset (around 2000 LST).

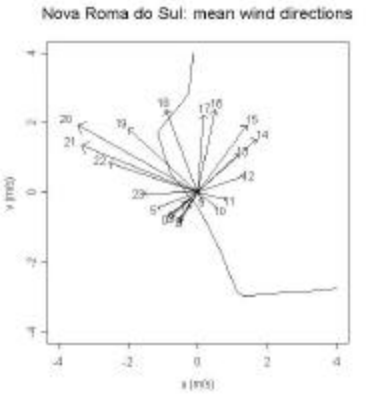

Figure 3. Average wind directions observed at Nova Roma do Sul for each hour of the daily cycle. The solid line indicates the location of the cliff.

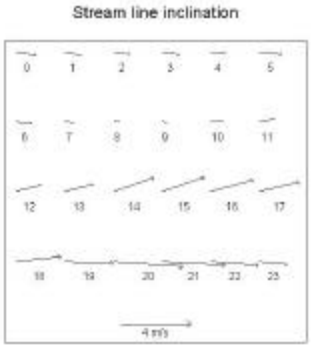

Figure 4. Average inclination of the mean stream line at each hour of the daily cycle, relative to the horizontal. The magnitude is given by the vector at the bottom.

3.2. *Mean quantities*

The minimum wind magnitude is observed at 0900 LST (figure 5a). This is the time when upslope winds start, confirming that the stronger winds at night are driven by the downward displacement of cold air. This is also the time when the stable stratification breaks (figure 5b). The early evening transition happens around 1800 LST, when the thermal stratification first becomes stable. A subtle humidity jump (Acevedo and Fitzjarrald, 2001) is observed at this time (figure 5c).

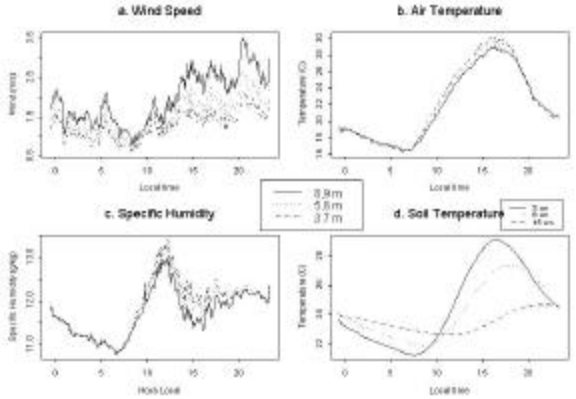

Figure 5. a. Average evolution of wind speed at each of the three levels, as given by legend; b. same as (a), but for air temperature; c. same as (a), but for specific humidity; d. same as (a), but for soil temperature.

3.3. *Turbulence parameters*

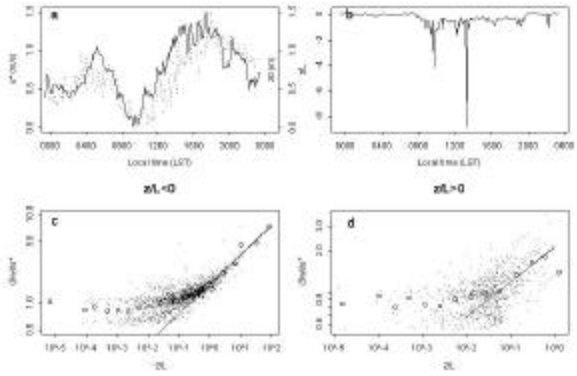

Figure 6. a. Average daily evolution of u_* (solid) and z_0 (dotted, scale on right axis); b. Same as (a), but for z/L; c. Ratio S_w/u_* as a function of z/L, for $z/L<0$. The solid line represents 1.65 (-z/L)^(1/3), circles are block averages; d. Same as (c), but for $z/L>0$ and solid line is 2.16 (z/L)^(1/4)

The turbulence intensity is a strong function of time of the day, as is the mean wind magnitude. The velocity scale u_* is maximum around 1800 LST, and minimum at 0900 LST (figure 6a). The cliff induces downslope winds at night, which keep the surface always turbulent in the period. In fact, even on clear nights, the surface was never observed to decouple

from the upper boundary layer. The roughness length also shows a clear daily cycle (figure 6a), very much in phase with that of u_*. This result suggests that z_0 is controlled by turbulent intensity, rather than by wind direction and the different types of land cover existent in the different directions upwind from the tower. The weakly stable state of the surface at night is shown by the average daily evolution of the stability parameter z/L (figure 6b), which only reaches very low positive values. In very convective conditions ($z/L < -0.1$), the ratio between the standard deviation of the vertical velocity perturbation (S_w) and u_* follows the 1/3 power of z/L (figure 6c), in agreement with previous studies (Stull, 1988). This ratio approaches unity in neutral conditions, while under more stable stratification ($z/L > 0.01$) it seems to behave as a 1/4 power of the stability parameter (figure 6d).

3.4. *Energy budget*

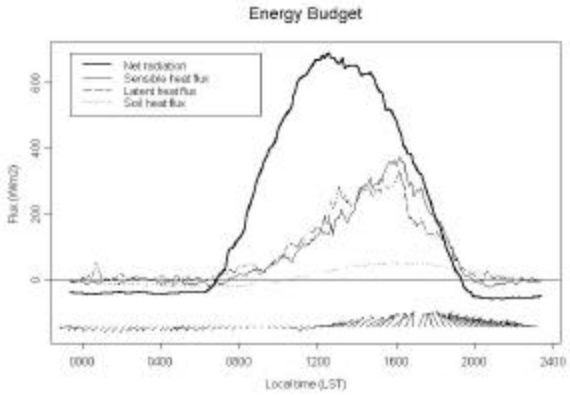

Figure 7. Average evolution of the energy budget components on ten clear days, as given by legend. Soil heat flux was measured at an 8-cm depth. Arrows at the bottom indicate the mean wind direction.

The vertical surface fluxes were determined after a 3-D rotation of the flow, so that the mean wind vector coincided with the u component, while w is the principal normal direction (Kaimal and Finnigan, 1994, p. 234). Sensible (H) and latent (LE) heat fluxes were determined from 30-minute data windows, to avoid the loss of low frequency fluxes (Sakai et. al., 2002). Even though net radiation peaks around 1300 LST, both H and LE peak later in the afternoon, around 1630 LST (figure 7). In fact, near sunset, each of the heat fluxes has itself a similar magnitude to that of net radiation. We speculate that it is caused by the direct exposition of the slope above which the tower is located to the solar radiation during the afternoon. Rotach et. al. (2000) show similar results in their slope measurements in the Alps.

The positive peak of the vertical heat fluxes seen in figure 7 coincides with a negative peak of the horizontal fluxes in the direction of the mean wind ($u'T'$ and $u'q'$, figure 8). At this period, there is a mean upslope wind (figures 3 and 4), which tends to bring colder, drier air, from levels disattached to the surface. The same horizontal fluxes are, in average, positive from 1700 to 2000 LST, when the mean wind blows from land. At night, $u'T'$ and $u'q'$ are larger in magnitude, than H and LE, respectively. In the same period, $u'T'$ remains negative, while $u'q'$ is positive, the expected behavior of the vertical fluxes. It suggests a downslope transport of colder, moister air by the mean wind at night.

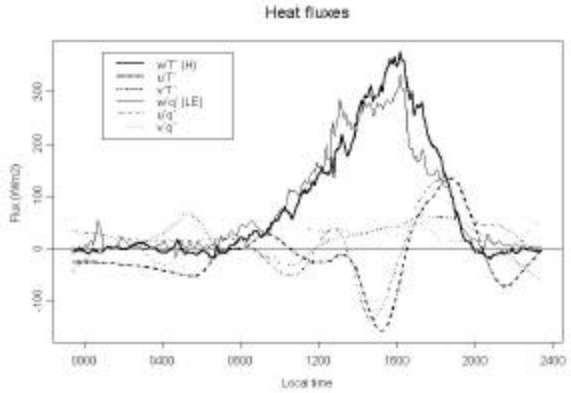

Figure 8. Average daily evolution of vertical and horizontal turbulent heat fluxes on ten clear days, as given by legend. Horizontal fluxes were smoothed for clarity.

Figure 7 shows that the Bowen ratio ($B=H/LE$) is not constant along the day, as $H<LE$ around noon and $H>LE$ in the afternoon. A possible explanation for that comes from the fact that the winds are blowing from different directions in the two periods and, therefore, the tower is "looking"at different types of surface. There is, indeed, a dependency of B on the inclination of the mean wind (figure 9). It tends to be larger for downslope wind, which blows from land than from upslope ones. In this case, the presence of the river may be determining larger LE, reducing the Bowen ratio.

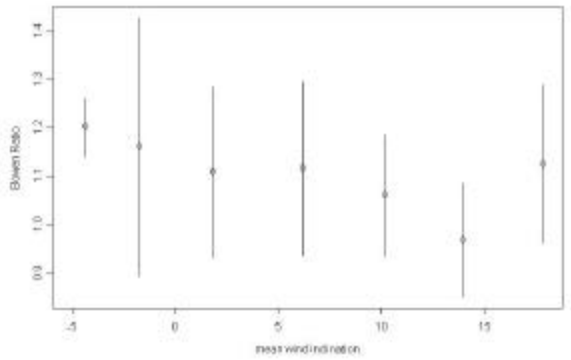

Figure 9. Average Bowen Ratio as a function of the inclination of the mean stream line. Vertical segments show the standard deviation for each class of data. The analysis includes only data from 0900 to 1900 LST.

4. CONCLUSIONS AND FUTURE WORK

We presented a number of observations taken at a micrometeorological tower located a few meters from a cliff, in southern Brazil. The presence of the cliff is felt in most of the variables. Mean circulations are totally controlled by the topography, downslope at night, becoming upslope when the stable stratification is broken at the surface. Very stable conditions never occur, a consequence of the constant nocturnal winds. Vertical surface fluxes peak in the middle of the afternoon, rather than at noon, probably due to the cliff slope direct exposition to solar radiation at the period. Horizontal fluxes are important for the local conditions. At night, the mean horizontal wind transports colder, moister air downward. On the other hand, the same fluxes show a negative peak roughly at the same time when the vertical fluxes are maximum. The different wind directions along the day seem also to affect the observed Bowen ratio, which tends to be larger with downslope winds

The results shown here are not yet complete. A careful analysis of the momentum vertical and horizontal fluxes is necessary, to understand the interaction of the cliff with the wind field.

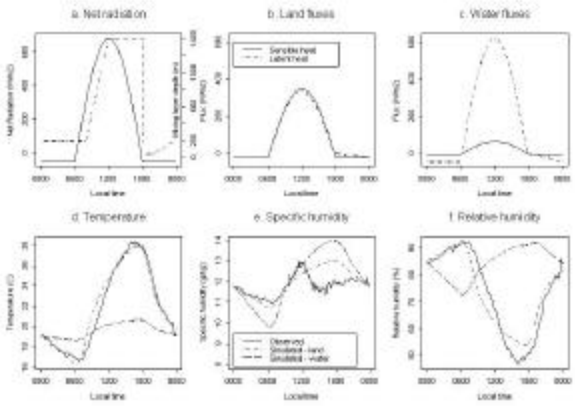

Figure 10. parameters of the energy partition model: a. Net radiation (solid) and mixed layer height (dashed, scale on righ axis); b. surface fluxes over land; c. surface fluxes over water, d. temperature evolution, according to legend on frame (e); e. same as (d), but for specific humidity; f. same as (d), but for relative humidity.

Another campaign is scheduled for May 2002. A second tower will be installed close to the river, with the purpose of explaining how the different surface types affect the fluxes. The final goal of this program is the estimation of the climatic impact of the river flooding, and the future observations will be helpful to that matter. So far, a very simple analysis based on the observed properties has been done. This is a simple energy partition model (figure 10), in which constant and changing Bowen ratios are assumed for land (figure 10b) and water (figure 10c). The latter is largely questionable, as the sensible heat flux over a body of water can even be negative, and we hope to clarify this matter with the addition of the tower close to the river. Assuming that the surface fluxes converge at the mixed layer, with a given entrainment rate, we estimate temperature (figure 10d) and specific humidity (figure 10e) for land and water. The close agreement of the observed temperature and the modelled evolutions for land was obtained with the adjustment of the mixed layer height (figure 10a). This way, one can use the water and land surface relative extensions before and after the flooding to determine how the average properties are affected in the region. This is a very preliminary analysis, which does not account for the real horizontal mixing by the local circulations, but only assumes that a whole region is horizontally mixed. We intend to use mesoscale atmospheric circulation models to simulate the climatic impact in more detail, determining how different regions are affected. The surface forcing of those simulations will be given by the observations discussed here.

ACKNOWLEDGEMENTS

This work was supported by CNPq, the Brazilian Science Foundation.

REFERENCES

Acevedo, O. C., and D. R. Fitzjarrald, 2001: The early evening surface layer transition: temporal and spatial variability, *J. Atmos. Sci*. **58**, No**.** 17, 2650-2667

Haugen, D. A., J. C. Kaimal, and E. F. Bradley, 1971: An experimental study of Reynolds stress and heat flux in the atmospheric surface layer. *Q. J. R. Meteorol.* Soc., **97**, 168-180.

Kaimal, J. C., and J. J. Finnigan, 1994: *Atmospheric boundary layer flows*. Oxford University Press, 289 pp.

Rotach, M. W., P. Calanca, R. Vogt, D. G. Steyn, S. Galmarini, J. Gurtz, 2000: The turbulence structure and exchange processes in an alpine valley: the MAP-Riviera project. Proceedings, 14th Synposium on Boundary Layer and Turbulence, Aspen, CO, Amer. Meteor. Soc, 380-383.

Sakai, R. K., D. R. Fitzjarrald, and K. E. Moore, 2001: Importance of low-frequency contributions to eddy fluxes observed over rough surfaces. *J. App. Meteorol*, **40**, No. 12, pp. 2178–2192.

Stull, R. B., 1988: *An introduction to boundary layer meteorology*. Kluwer Academic Publishers, 664 pp.